

Matrix Filters for the Detection of Extragalactic Point Sources in Cosmic Microwave Background Images

Diego Herranz and José Luis Sanz

Abstract—In this paper we introduce a new linear filtering technique, the so-called matrix filters, that maximizes the signal-to-interference ratio of compact sources of unknown intensity embedded in a set of images by taking into account the cross-correlations between the different channels. By construction, the new filtering technique outperforms (or at least equals) the standard matched filter applied on individual images. An immediate application is the detection of extragalactic point sources in Cosmic Microwave Background images obtained at different wavelengths. We test the new technique in two simulated cases: a simple two-channel case with ideal correlated color noise and more realistic simulations of the sky as it will be observed by the LFI instrument of the upcoming ESA's Planck mission. In both cases we observe an improvement with respect to the standard matched filter in terms of signal-to-noise interference, number of detections and number of false alarms.

Index Terms—Radio astronomy, Filters, Image enhancement, Image processing, Matched filters, Object detection

I. INTRODUCTION

THE detection of faint pointlike sources is a task that is common to many branches of Astronomy, from the search for protostars in gas-rich nebulae to the study of active galactic nuclei in the confines of the observable universe. Since the angular size of these objects is smaller than the angular resolution of the telescopes that are used to observe them, they appear as *point sources* with the shape of the telescope point spread function.

A case of particular interest is the detection of extragalactic point sources (EPS) in microwave wavelengths. In the microwave range of the electromagnetic spectrum, the sky is dominated by the so-called Cosmic Microwave Background (CMB) radiation, a relic of the hot and dense first moments of the universe. The study of the CMB is one of the hottest research topics in modern Cosmology. For a short review on the CMB, see [1]. The CMB signal is mixed with other signals of astrophysical origin, mainly the emission from our own Galaxy and from a large number of extragalactic objects including radio galaxies, dusty galaxies and galaxy clusters. For the typical angular resolution of current CMB experiments, ranging from a few arcmin to one degree, most of these extragalactic objects appear as point sources. From the standpoint of CMB, these point sources are contaminants that

must be removed; from the standpoint of extragalactic Astronomy, however, they provide a valuable source of information, particularly at microwave wavelengths where the properties of sources are poorly understood [2]. In both cases, techniques for the detection of faint point sources are needed.

For single images taken at a given wavelength the problem is equivalent to the general problem of detecting a number of objects, all of them with a known waveform but unknown positions and intensities, embedded in additive noise (not necessarily white). In the field of microwave Astronomy, wavelet techniques [3]–[7], Bayesian approaches [8], [9], matched filters [10]–[12] and other related linear filtering techniques [13]–[19] have proved to be useful. The common feature of all these techniques is that they rely on the prior knowledge that the sources have a distinctive spatial behaviour (i.e. a known spatial profile, plus the fact that they appear as compact objects as opposed to ‘diffuse’ random fields) that helps to distinguish them from the noise.

Most of the current CMB experiments are able to observe the sky at several different wavelength bands. In particular, the Wilkinson Microwave Anisotropy Probe (WMAP) [20], [21] is observing the sky at 23, 33, 41, 61 and 94 GHz and the upcoming ESA's Planck satellite [22] will observe the sky in nine frequency channels ranging from 30 to 857 GHz. Multi-wavelength data can be used to improve the detection/separation of astrophysical components. For example, CMB can be separated from Galactic dust and synchrotron emission using well-established methods; a non-exhaustive list of them include Independent Component Analysis [23], [24], Maximum Entropy Method [25]–[27], Internal Linear Combination [20], [28] and Wiener filtering [29], among others. Moreover, specific techniques for the detection of compact sources whose spectral behaviour is well known have been proposed in the literature; a typical example is the detection of the so-called Sunyaev-Zel'dovich effect due to galaxy clusters [30]–[33].

All the previous component separation techniques, however, are in trouble when dealing with extragalactic point sources. EPS form a very heterogeneous population constituted by a large number of objects with very different physical properties, from radio-emitting active galactic nuclei to dusty star-forming galaxies. Since each source is a unique object, with an spectral emission law that is different from the spectral emission law of any other, the component separation problem is underdetermined: the number N of components to be separated is much larger than the number M of channels available. Attempts to

D. Herranz and J.L. Sanz are with the Astronomy Department, Instituto de Física de Cantabria, CSIC-UC, Av. los Castros s/n, 39005 Santander, Spain, e-mail: herranz@ifca.unican.es. J.L. Sanz is currently on a sabbatical year at the ISTI (CNR), Pisa, Italy.

Manuscript received —; revised —.

simplify the problem by grouping the extragalactic sources into classes of objects with similar spectral behaviour are in most cases unsatisfactory.

So far we have considered two approaches: on the one hand, it is still possible to work channel by channel, separately, by using the filtering techniques above mentioned. But in that case a valuable fraction of the information that multi-wavelength experiments can offer is wasted. On the other hand, standard multi-wavelength component separation techniques are impracticable because the number of physical components involved is too high. An intermediate approach is to design filters that are able to find compact sources thanks to their distinctive spatial behaviour while at the same time do incorporate some multi-wavelength information, without pretending to achieve a full component separation. In this paper we propose a new filtering technique that makes no assumptions about the spectral behaviour of the sources, but that makes use of some multi-wavelength considerations, namely:

- When a source is found in one channel, it will be also present in the same position in all the other channels.
- The spatial profile of the sources may differ from channel to channel, but it is a priori known. For example, for a microwave experiment the source profile is equal to the antenna response of the experiment's radiometers¹, that is well known.
- The second order statistics of the background in which the sources are embedded is well known or it can be directly estimated from the data by assuming that point sources are sparse.

We find that the new technique we propose takes the form of a matrix of filters that can be applied to any number M of channels. In the case of a single channel, the matrix of filters defaults to the standard matched filter. In section II we will introduce the new formalism. In section III we will illustrate the new method with two different tests: a simple toy model and a more realistic simulation that corresponds to a small region of the sky as it will be observed by the upcoming Planck mission. Finally, in section IV we will draw some conclusions.

II. MATRICES OF FILTERS

A. Data model

Let us consider an experiment whose outcome is a set of N two-dimensional images (channels) where there are embedded a unknown number of point sources. For simplicity, let us consider the case of a single point source located at the origin of the coordinates. Our data model is

$$D_k(\vec{x}) = s_k(\vec{x}) + n_k(\vec{x}), \quad (1)$$

where the subscript $k = 1, \dots, N$ denotes the index of the image. The term $s_k(\vec{x})$ denotes the point source,

$$s_k(\vec{x}) = A_k \tau_k(\vec{x}). \quad (2)$$

In the previous equation A_k is the unknown amplitude of the source in the k^{th} channel and $\tau_k(\vec{x})$ is the spatial profile of the

source and satisfies the condition $\tau_k(\vec{0}) = 1$. We consider that the τ_k are known a priori, as is the case in most experiments in Astronomy. For the case of point sources, each τ_k is just the beam response (normalised to one) of the telescope for the k^{th} channel.

The term $n_k(\vec{x})$ in equation (1) is the noise in the k^{th} channel. It contains not only instrumental noise, but also other astrophysical components apart from the point sources. In the case of Microwave Astronomy, for example, $n_k(\vec{x})$ is the combination of the CMB, Galactic emission (due to Galactic dust, synchrotron, etc) and the instrumental noise. Since the N images correspond to the same area of the sky observed at different wavelengths, the astrophysical components are correlated among the different channels. Let us suppose the noise term can be characterized by its cross-power spectrum:

$$\langle n_k(\vec{q}) n_l^*(\vec{q}') \rangle = P_{kl}(\vec{q}) \delta^2(\vec{q} - \vec{q}'), \quad (3)$$

where $\mathbf{P} = (P_{kl})$ is the cross-power spectrum matrix and n^* is the complex conjugate of n . Besides, we assume that the noise has zero mean,

$$\langle n_k(\vec{x}) \rangle = 0. \quad (4)$$

B. Matrix filters

Let $\Psi_{kl}(\vec{x})$ be a set of $N \times N$ linear filters, and let us define the set of quantities

$$\begin{aligned} w_k(\vec{x}) &= \sum_l \int d\vec{x}' \Psi_{kl}(\vec{x} - \vec{x}') D_l(\vec{x}') \\ &= \sum_l \int d\vec{q} e^{-i\vec{q} \cdot \vec{x}} \Psi_{kl}(\vec{q}) D_l^*(\vec{q}). \end{aligned} \quad (5)$$

The quantity w_k in equation (5) is, therefore, the sum of a set of linear filterings of the data D_l . The last term of the equation is just the expression of the filterings in Fourier space, being \vec{q} the Fourier mode and $\Psi_{lk}(\vec{q})$ and $D_l(\vec{q})$ the Fourier transforms of $\Psi_{kl}(\vec{x})$ and $D_l(\vec{x})$, respectively.

We intend to use the combined filtered images $w_k(\vec{x})$ as estimators of the source amplitudes A_k . For that purpose, we require that the filters Ψ_{kl} satisfy the condition:

$$\langle w_k(\vec{0}) \rangle = A_k, \quad (6)$$

that is, that the k^{th} combined filtered image at the position of the source is, on average over many realizations, an *unbiased* estimator of the amplitude of the source in the k^{th} channel. Using equation (5), this condition can be expressed as

$$A_k = \sum_l \int d\vec{q} \Psi_{kl}(\vec{q}) A_k \tau_l^*(\vec{q}). \quad (7)$$

The previous condition is automatically satisfied if

$$\int d\vec{q} \Psi_{kl}(\vec{q}) \tau_l^*(\vec{q}) = \delta_{kl}. \quad (8)$$

This condition establishes that for a fixed image k the filter component Ψ_{kk} is sensitive to the signal whereas the other components Ψ_{kl} , $k \neq l$, do not affect the signal and are sensitive only to the noise. A similar idea was proposed by [34] in the context of the extraction of the Rees-Sciama effect

¹In general, of its detectors. Some microwave experiments use bolometers instead of radiometers, but the distinction is irrelevant for the purposes our discussion.

where, on the the way around, the filter was defined to be orthogonal to a noise component.

We want to estimators w_k to be not only unbiased, but *efficient* as well. Then we need to minimize the variance σ_{w_k} of the combined filtered image. It is straightforward to show that

$$\sigma_{w_k}^2 = \sum_l \sum_m \int d\vec{q} \Psi_{kl}(\vec{q}) \Psi_{km}^* P_{lm}(\vec{q}). \quad (9)$$

In order to obtain the filters that satisfy condition (8) and at the same time minimize equation (9) for all k , we solve simultaneously the constrained minimization problem given by the Lagrangians \mathcal{L}_k , $k = 1, \dots, N$:

$$\begin{aligned} \mathcal{L}_k = & \sum_{l,m} \int d\vec{q} \Psi_{km}^* P_{lm} \Psi_{kl} - \\ & 2 \sum_l \lambda_{kl} \left[\int d\vec{q} \Psi_{kl} \tau_l^* - \delta_{kl} \right], \end{aligned} \quad (10)$$

where the functional dependence on \vec{q} of the quantities Ψ , τ and P has been omitted for simplicity and where the λ_{kl} is a set of Lagrangian multipliers. The solution of this problem is given by the matrix equation

$$\Psi^* = \mathbf{F} \mathbf{P}^{-1}, \quad (11)$$

where

$$\mathbf{F} = (F_{kl}), \quad \mathbf{P} = (P_{kl}), \quad \lambda = (\lambda_{kl}), \quad \mathbf{H} = (H_{kl}), \quad (12)$$

and where

$$\begin{aligned} F_{kl} &= \lambda_{kl} \tau_l, \\ \lambda &= \mathbf{H}^{-1}, \\ H_{kl} &= \int d\vec{q} \tau_k(\vec{q}) P_{kl}^{-1} \tau_l^*(\vec{q}). \end{aligned} \quad (13)$$

In the particular case where $P_{kl} = \delta_{kl} P_k$, that is, where the noise is totally uncorrelated among channels, it can be seen that the elements of the matrix of filters default to

$$\Psi_{kl}^*(\vec{q}) = \delta_{kl} \frac{\tau_k(\vec{q}) / P_k(\vec{q})}{\int d\vec{q} \tau_k^2(\vec{q}) / P_k(\vec{q})}. \quad (14)$$

In that case the matrix of filters defaults to a diagonal matrix whose non-zero elements are the complex conjugates of the matched filters that correspond to each channel. In the case of circularly symmetric source profiles and statistically homogeneous and isotropic noise, the filters are real-valued and the whole process is equivalent to filter each channel independently with the appropriate matched filter. In fact, the matched filter for the k -th channel is exactly given by the right side of equation (14), not considering the delta symbol. The matched filter is known to be the optimal linear filter (that is, the one that gives maximum signal to noise amplification) for an individual image. For more information about matched filters in the context of point source detection in CMB astronomy, see [10]–[12] and references therein.

C. Relation to other multi-wavelength approaches

As mentioned in the introduction, some other filtering techniques have been proposed in the literature for the problem of detecting compact sources in multi-wavelength astronomical data sets. The crucial difference is that while in all the previous approaches the spectral behaviour of the sources must be known *a priori*, here we do not assume any prior knowledge about it. Of course, if the spectral behaviour is perfectly known (as it is the case of the Sunyaev-Zel'dovich effect of galaxy clusters) this knowledge can be used to greatly improve the power of the filtering. But if there is any uncertainty in the spectral behaviour of the sources, or if the spectral behaviour varies from one source to another (as it is the case of extragalactic point sources), the robustness of the method is in great peril.

The so called *matched multifilters* [30], [32], [33] is one of the most commonly used multi-wavelength filtering technique. It is, in its derivation, a close relative of the matrix filters proposed here. Whereas for the matrix filters we have a $N \times N$ matrix of filters that are used to produce N filtered maps, in the case of matched multifilters we have N filters that are used to produce one single, combined filtered map. The reduced dimensionality of the matched multifilter solution is a direct consequence of the fact that all the sources in the image are assumed to have exactly the same spectral behaviour. The variance of this single filtered map is given by equation (22) of [30] (see that paper for a complete description of matched multifilters).

In order to illustrate the differences between both methods, let us imagine a very simplistic case, consisting of two images A and B that contain white noise with identical variances σ^2 . Let us assume that the noise in A is totally uncorrelated with the noise in B and that we place two identical sources at the same coordinates of A and B. Images A and B can then be considered as two different ‘channels’ of an ideal experiment with a point source that has a perfectly flat spectral behaviour. According to equations (9) and (14) the output of the matrix filters would be *two* images, each one filtered with the equivalent of a single band matched filter; both images will have identical variances $\sigma_w^2 < \sigma^2$. If, on the other hand, we use matched multifilters (provided we know the correct spectral behaviour) it can be seen from equation (22) of [30] that the output would be a *single* map with variance $\sigma_{MMF}^2 = \sigma_w^2/2$. This simple example serves to illustrate that matched multifilters are more powerful than matrix filters, provided the spectral behaviour is well known².

Conversely, if the spectral behaviour is not known then the matched multifilters are biased (they do not recover the correct amplitude of the sources), whereas matrix filters are unbiased independently of the degree of knowledge of the spectral behaviour.

²Of course, things are not that simple: in this very example, if the spectral behaviour is really known one could always perform a linear combination of the two uncorrelated output maps produced by the matrix filters in order to produce a final map with the same $\sigma_w^2/2$ variance: the key point is not the choice of filters, but the knowledge of the spectral behaviour.

D. Extension to the sphere

The previous formulas have been derived for the case of flat two-dimensional images such as the ones corresponding to a small patch of the sky. It is straightforward to extend them to the spherical case (i.e. the full sky), just by using harmonic instead of Fourier transforms. Note, however, that the Galactic foregrounds vary strongly across the sky, and therefore it may be wiser to work locally in small areas of the sky (that can be safely projected into the tangent plane in order to get ordinary flat images), where the spatial variation of the foregrounds is not so drastic. This is the approach already used in most point source detection applications in the literature [7], [12], [15], [16].

III. NUMERICAL TESTS

In this section we will test the matrix filters in two different kind of simulations. In both cases we will compare the performance of the new matrix filters with the performance of the standard matched filter applied to the individual images. The matched filter is the optimal linear filter for individual images; therefore, any improvement with respect to the matched filter will prove the usefulness of including multi-wavelength information in our scheme. Other possibility would have been to compare with wavelet filters such as the Mexican Hat Wavelet that have been widely used in the literature [3]–[5], [7]. In [12] it has been shown, however, that wavelet filters perform very similarly to matched filters (with a subtlety here: wavelet filters are suboptimal in the sense of signal to noise amplification, but their implementation is generally easier and more robust to highly contaminated images. Both effects tend to roughly compensate one with the other, leading to an almost identical performance). Therefore, and in order to keep things simple, in this work we will compare the new technique only with standard matched filters.

The two cases we will consider are as follows. The first case will be a toy model simulation with only two channels and very simple noise and it will serve to illustrate the method. The second case consists of a more realistic simulation of a small patch of the sky as will be observed with the LFI (Low Frequency Instrument) of the upcoming Planck mission.

A. Toy model simulations

For this test we keep the things simple and simulate only a hypothetic two-channels, ideal experiment. Each simulation consists of two images, which we will call ‘image A’ and ‘image B’ respectively. Image A contains random color noise with power spectrum $P(q) \propto q^{-2.5}$. For the image B we generate a random color noise with power power spectrum $P(q) \propto q^{-0.5}$ and, since we are interested in the case where there is some correlation between the two images, then we add to it the first map multiplied by 0.5. For simplicity, we normalise both images to unit variance (in arbitrary units). The result are two correlated random noises with correlation factor 0.67. We add a Gaussian-shaped source with an intensity that is randomly distributed in the interval (2.75, 3.75) (in the same arbitrary units of the map) and $FWHM = 3.33$ pixels to image A. At the same position in image B we simulate

a Gaussian-shaped source with a different random intensity (uniformly drawn from the same interval) and $FWHM = 10$ pixels³. An example is shown in the top panels of Fig. 1. We perform 250 of these simulations.

Each pair of images A and B are filtered with the matrix filters in equation (11). In parallel, each single image is filtered with its corresponding matched filter (MF). Examples are shown in the middle and bottom panels of Fig. 1. Note that, in the figure, the filtered images generated by the matrix filters and the matched filter are very similar for image A, but quite different for image B.

We are interested in increasing the signal-to-interference ratio (SIR) of the sources. Let us define the SIR gain or “amplification” of a filter (or set of filters) as the ratio between the SIR of the source after filtering and the SIR of the source before filtering. A higher amplification factor means a better chance of detecting a source. Fig. 2 shows the gain factors (in dB) achieved by matrix filters versus the gains given by standard matched filters for images A and B. For the case of A images the ratio between the gain obtained with the matrix filters and the gain obtained with the matched filters is small, only 1.03 on average, whereas for the case of B images the ratio between the two gain factors is (again on average) 1.34, which means a significant improvement of the final SIR of the sources. This implies that if we had fixed a given detection threshold, the same for the two filtering techniques, with the matrix filters we would have been able to detect sources 0.7 times less intense than with the matched filter.

We are interested as well in obtaining a good estimation of the intensity of the sources. In Fig. 3 the histograms of the relative error in the estimation of the source intensities are shown for images A and B and for matrix filters and matched filters. The relative error is defined as $e = 100 \times (I_0 - I_e)/I_0$, where I_0 is the input intensity and I_e is the estimated intensity (the central intensity after filtering). For the case of A images the two histograms practically overlap, but for the case of B images the histogram corresponding to matched filter spreads more, indicating that intensity estimation with matched filters is less reliable than with matrix filters. A more quantitative measurement of the relative errors in each case is given by the dispersion of the error distribution shown in Fig. 3. For image A it is 9.2% and 9.6% for the matrix filters and the matched filter, respectively. For image B difference is more evident: 5.9% and 9.7% for the matrix and the matched filters, respectively.

Note that this toy example is not realistic at all from the point of view of Astronomy. For example, in a real observation of the sky the incoming signal from astronomical objects would be filtered by the telescope beam profile, that is not considered here. However, this example is meant only for academic and illustrative purposes. The effect of the telescope beam would have changed only the quantitative results (as the input images would have been somewhat different from the images we have used), but the qualitative behaviour of the

³These values have been chosen by chance: any other combination could serve us equally well for this exercise. The specific numerical results of the exercise depend on the sizes of the source profiles, but the qualitative behaviour of the method does not.

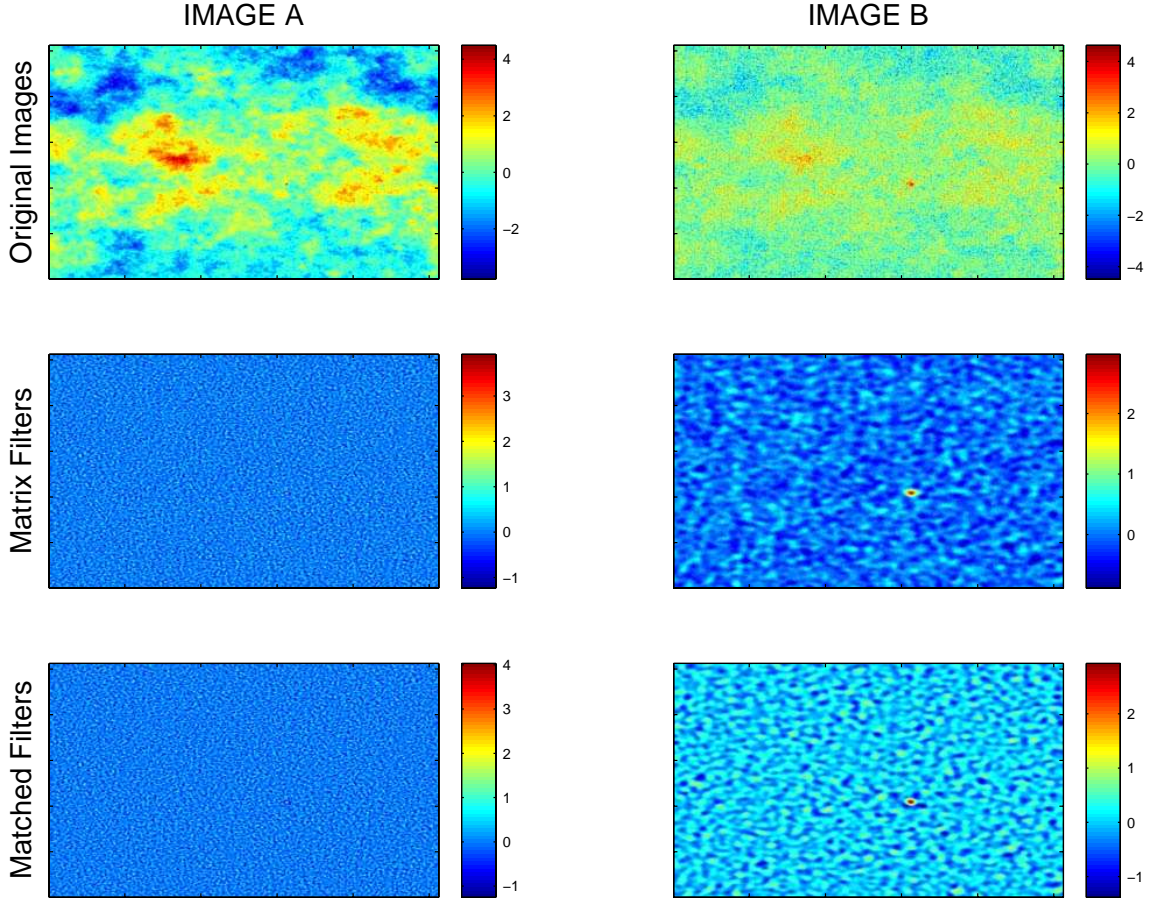


Fig. 1. One of the simulations used in the toy model test. Top panels: images A and B before filtering. Middle panels: images A and B after filtering with the matrix filters. Bottom panels: images A and B after filtering with the matched filter that corresponds to each case.

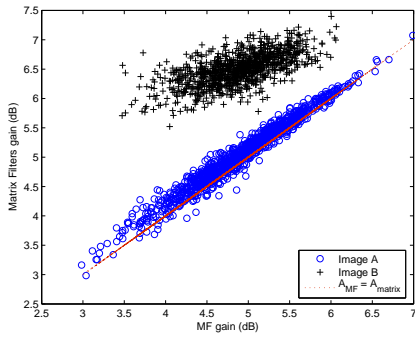


Fig. 2. SIR gain of matrix filters versus the SIR gain of standard matched filters for the 250 simulations in our test. Blue circles refer to images A and black crosses refer to images B. The red solid line shows the amplification factor of a filter with the same gain factor as the matched filter.

filters would have been the same.

B. Planck simulations

In order to further test the applicability of matrix filters to the detection of extragalactic objects in microwave Astronomy, we will now use realistic simulations of the sky as it will be observed by the ESA's Planck satellite. Again, the goal is to

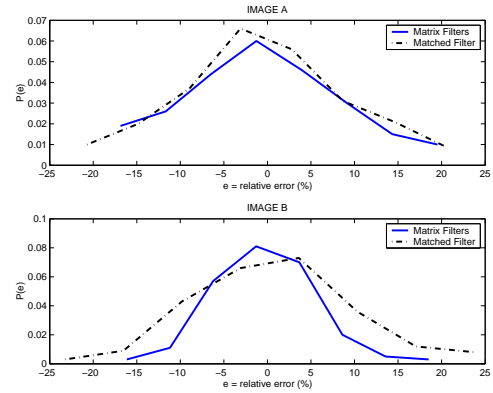


Fig. 3. Relative errors in the determination of the central intensity of the sources for image A (top panel) and B (bottom panel) after filtering with the matrix filters (solid blue line) and the standard matched filter (dash-dotted black line).

compare the performances of matrix filters and the standard matched filter.

For this test, we use the “Planck Reference Sky” simulations⁴ of the Low Frequency Instrument (LFI) Planck

⁴A set of state-of-the-art simulations developed by the Planck Working Group 2 for the technical and scientific preparation of the Planck mission.

channels: 30, 44 and 70 GHz. The simulations include the following astrophysical components: CMB, Galactic synchrotron, free-free and dust emission, thermal Sunyaev-Zel'dovich effect from galaxy clusters, radio galaxies and infrared dusty galaxies. Besides, the simulations include instrumental noise at the levels expected for the Planck detectors. We have selected a region of the sky centered at the Galactic North Pole. At LFI wavelengths and at high Galactic latitude the dominant astrophysical component is CMB, with a small contamination from synchrotron emission. Regarding extragalactic objects, the dominant population at this wavelengths is the one formed by radio galaxies. For a more detailed discussion about the the Planck Reference Sky simulations and the astrophysical components in them, see [12] and references therein.

The region of the sky we have selected covers an area of $14.66 \times 14.66 \text{ deg}^2$ of the sky, divided into 512×512 pixels of size $1.71 \times 1.71 \text{ arcmin}^2$. The antenna FWHM for the 30, 44 and 70 GHz channels are 33, 24 and 14 arcmin, respectively. Image units are expressed in MJy/sr⁵. The images are shown in the left panels of Fig. 4. Note that point sources are very difficult to see in the images. For the sake of clarity, the sources alone are shown in the second column of panels of Fig. 4.

We have filtered the images with the matrix filters and with the standard matched filter. The filtered images are shown in the third and fourth column of Fig. 4, respectively. For different detection thresholds and for both filters we have calculated the number of detected sources and the number of false alarms. The results are shown in Figs. 5, 6 and 7. For the three channels, matrix filters consistently give a higher number of true detections for a fixed number of false alarms. For all the considered cases, the positive detection rate over the minimum considered detection threshold is equal to one, that is: we detect all the sources we put in the simulation.

Another indicator of quality is the completeness flux, that is, the threshold above which all the input sources are detected. For the matrix filters, completeness fluxes are 0.16, 0.19 and 0.58 Jy for the 30, 44 and 70 GHz channels, respectively. For the matched filter, completeness fluxes are 0.32, 0.40 and 0.58 Jy for the same channels. This means that in two of the three channels considered matrix filters are able to detect fainter point sources than the matched filter. In the 70 GHz channel matrix filters reaches the same flux limit than the matched filter, but from Fig. 7 it is clear that for a fixed number of false alarms they lead to a higher number of positive detections.

IV. CONCLUSION

In this work we have introduced a new filtering technique, the matrix filters, that can be of utility for the detection of extragalactic point sources in multi-wavelength experiments of the Cosmic Microwave Background. Matrix filters are designed to maximize the signal-to-interference ratio of compact sources embedded in a set of images ("channels") by taking into account the cross-correlations between the different channels. For the case of a single-channel experiment and circularly

symmetric sources, the matrix of filters defaults to the standard matched filter. For the case of M totally uncorrelated channels and circularly symmetric sources, the matrix of filters becomes a diagonal matrix whose non-zero elements are the matched filters corresponding to each channel. In a general case, the non diagonal elements of the matrix are non zero. Since the matrix filters contain as a particular case the matched filter and they are designed to maximize the signal-to-interference ratio, then the individual amplifications for each channel (defining by amplification the quotient between the signal-to-interference ratios after and before filtering) are greater or (in the worst case) equal to the amplifications obtained by the standard matched filters.

We have tested the matrix filters in two simulated cases: a simplistic two-channel case with ideal noise and a more realistic simulation of the sky as it will be observed by the LFI instrument of the upcoming ESA's Planck mission. In the first test we observe that matrix filters clearly outperform the standard matched filter for one of the channels, while for the other channel their performance is very similar to that of the matched filter. Other simulation tests with different parameters we have carried out show a similar behaviour: there is a significant gain for at least one of the channels with respect to standard matched filters.

For the second test case we have considered one single patch of the sky, observed at 30, 44 and 70 GHz. The purpose of this test was just to give an example of how the matrix filters work in a more realistic case. In this example, matrix filters outperform the matched filter both in the flux limit they can reach and in the ratio between false alarms and true detections. This result seems to indicate that matrix filters could help to obtain better catalogues of extragalactic point sources in future CMB experiments. However, this result has been obtained for a single simulation of a small portion of the sky, and therefore it may not be extrapolable to the whole sky or to any other experiment. The study of the application of matrix filters to the whole microwave sky for the Planck mission is the subject of a future work.

ACKNOWLEDGMENT

The authors acknowledge partial financial support from the Spanish Ministry of Education (MEC) under project ESP2004-07067-C03-01 and from the joint CNR-CSIC research project 2006-IT-0037. JLS, on sabbatical leave, acknowledges financial support from the Spanish Ministry of Education and thanks the CNR ISTI for the hospitality during the sabbatical. We would like to thank J. González-Nuevo and M. López-Cañiego for useful comments.

REFERENCES

- [1] D. Scott and G. Smoot, "Cosmic Microwave Background Mini-Review," *ArXiv Astrophysics e-prints*, astro-ph/0601307, Jan. 2006.
- [2] The Planck Collaboration, "The Scientific Programme of Planck," *ArXiv Astrophysics e-prints*, astro-ph/0604069, Apr. 2006.
- [3] P. Vielva, R. B. Barreiro, M. P. Hobson, E. Martínez-González, A. N. Lasenby, J. L. Sanz, and L. Toffolatti, "Combining maximum-entropy and the Mexican hat wavelet to reconstruct the microwave sky," *Monthly Notices of the Royal Astronomical Society*, vol. 328, pp. 1–16, Nov. 2001.

⁵In radio astronomy, the flux unit or jansky (symbol Jy) is a non-SI unit of electromagnetic flux density equivalent to 10^{-26} watts per square metre per hertz. The unit is named after the pioneering radio astronomer Karl Jansky.

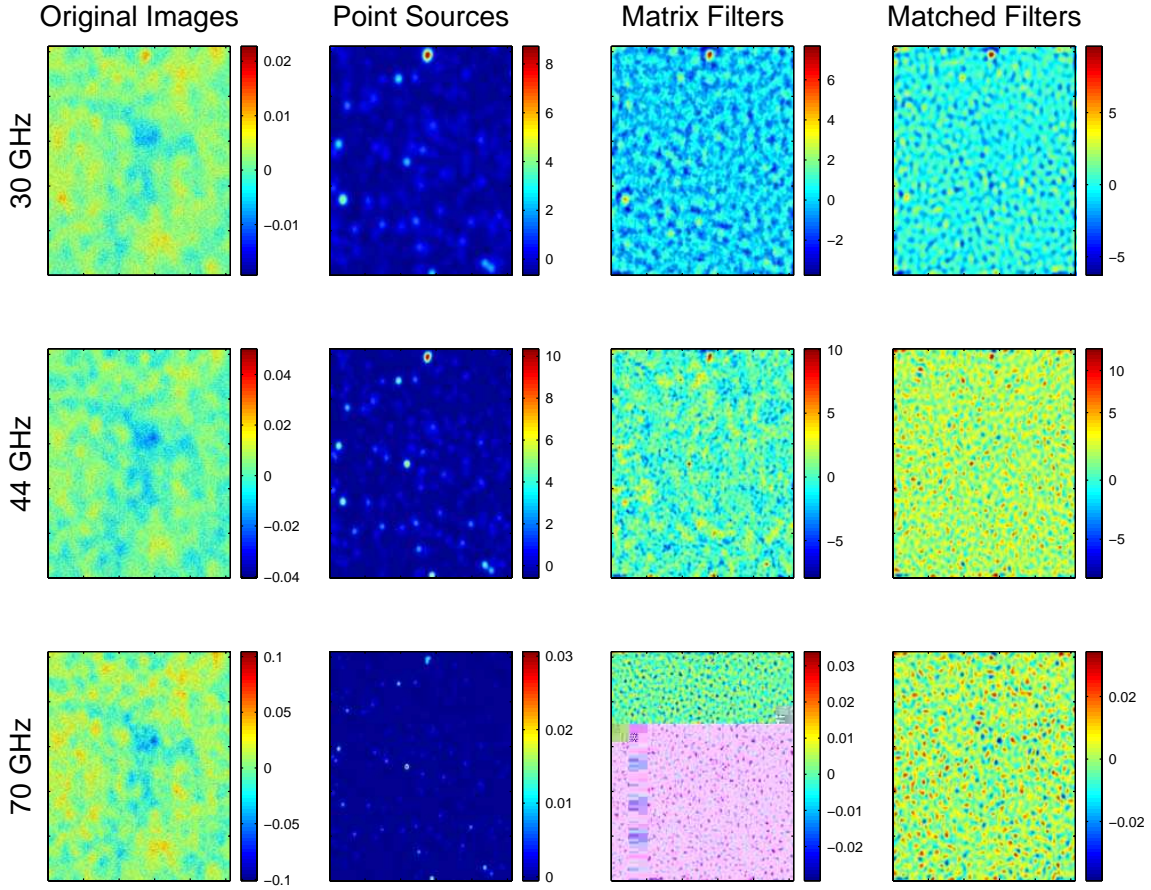


Fig. 4. Planck simulations. Left panels: the original images, including point sources. The channels shown are, from top to bottom, 30, 44 and 70 GHz. Second column of panels from the left: the point sources alone. Third column from the left: images filtered with the matrix filters. Fourth column from the left: images filtered with the matched filter.

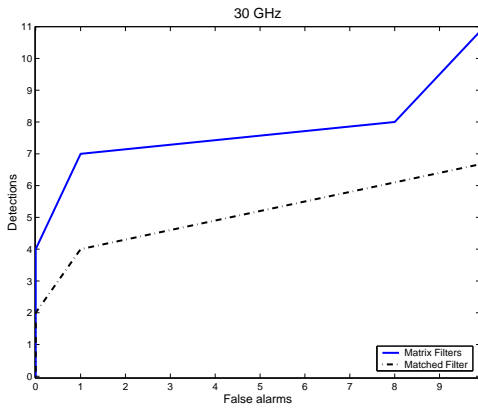


Fig. 5. Number of detected sources as a function of the number of false alarms for the matrix filters (solid blue line) and the matched filter (dash-dotted black line), for the 30 GHz channel.

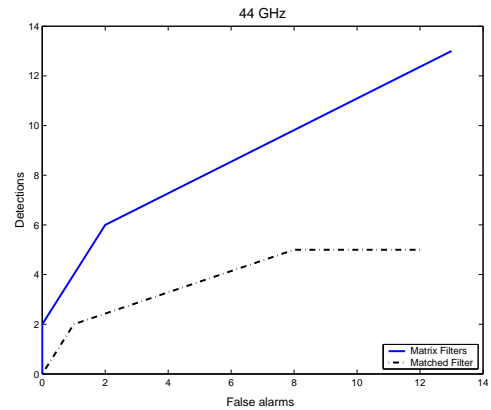


Fig. 6. Number of detected sources as a function of the number of false alarms for the matrix filters (solid blue line) and the matched filter (dash-dotted black line), for the 44 GHz channel.

- [4] P. Vielva, E. Martínez-González, J. E. Gallegos, L. Toffolatti, and J. L. Sanz, "Point source detection using the Spherical Mexican Hat Wavelet on simulated all-sky Planck maps," *Monthly Notices of the Royal Astronomical Society*, vol. 344, pp. 89–104, Sep. 2003.
- [5] J. González-Nuevo, F. Argüeso, M. López-Caniego, L. Toffolatti, J. L. Sanz, P. Vielva, and D. Herranz, "The Mexican hat wavelet family: application to point-source detection in cosmic microwave background maps," *Monthly Notices of the Royal Astronomical Society*, vol. 369, pp. 1603–1610, Jul. 2006.
- [6] J. L. Sanz, D. Herranz, M. López-Caniego, and F. Argüeso, "Wavelets on the sphere. Application to the detection problem," in *Proceedings of the 14th European Signal Processing Conference (2006)*, ser. EUSIPCO 2006 Conference, Sep. 2006, pp. 1–5.
- [7] M. López-Caniego, J. González-Nuevo, D. Herranz, M. Massardi, J. L. Sanz, G. De Zotti, L. Toffolatti, and F. Argüeso, "Nonblind Catalog of Extragalactic Point Sources from the Wilkinson Microwave Anisotropy Probe (WMAP) First 3 Year Survey Data," *The Astrophysical Journal Supplement Series*, vol. 170, pp. 108–125, May 2007.

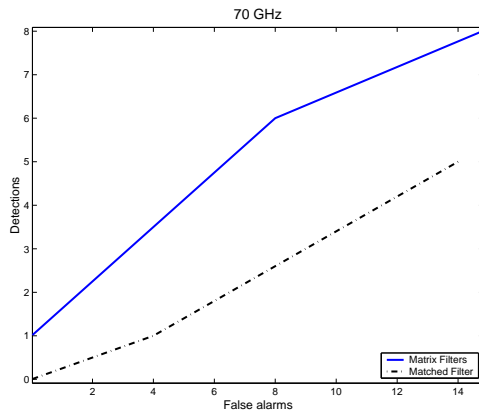


Fig. 7. Number of detected sources as a function of the number of false alarms for the matrix filters (solid blue line) and the matched filter (dash-dotted black line), for the 70 GHz channel.

- [8] M. P. Hobson and C. McLachlan, "A Bayesian approach to discrete object detection in astronomical data sets," *Monthly Notices of the Royal Astronomical Society*, vol. 338, pp. 765–784, Jan. 2003.
- [9] P. Carvalho, G. Rocha, and M. P. Hobson, "A fast Bayesian approach to discrete object detection in astronomical datasets - PowellSnakes I," *ArXiv e-prints*, *arXiv:0802.3916v1*, vol. 802, Feb. 2008.
- [10] M. Tegmark and A. de Oliveira-Costa, "Removing Point Sources from Cosmic Microwave Background Maps," *Astrophysical Journal Letters*, vol. 500, pp. L83+, Jun. 1998.
- [11] R. B. Barreiro, J. L. Sanz, D. Herranz, and E. Martínez-González, "Comparing filters for the detection of point sources," *Monthly Notices of the Royal Astronomical Society*, vol. 342, pp. 119–133, Jun. 2003.
- [12] M. López-Cañiego, D. Herranz, J. González-Nuevo, J. L. Sanz, R. B. Barreiro, P. Vielva, F. Argüeso, and L. Toffolatti, "Comparison of filters for the detection of point sources in Planck simulations," *Monthly Notices of the Royal Astronomical Society*, vol. 370, pp. 2047–2063, Aug. 2006.
- [13] J. L. Sanz, D. Herranz, and E. Martínez-González, "Optimal Detection of Sources on a Homogeneous and Isotropic Background," *The Astrophysical Journal*, vol. 552, pp. 484–492, May 2001.
- [14] L.-Y. Chiang, H. E. Jørgensen, I. P. Naselsky, P. D. Naselsky, I. D. Novikov, and P. R. Christensen, "An adaptive filter for the construction of the Planck Compact Source Catalogue," *Monthly Notices of the Royal Astronomical Society*, vol. 335, pp. 1054–1060, Oct. 2002.
- [15] D. Herranz, J. L. Sanz, R. B. Barreiro, and E. Martínez-González, "Scale-adaptive Filters for the Detection/Separation of Compact Sources," *The Astrophysical Journal*, vol. 580, pp. 610–625, Nov. 2002.
- [16] D. Herranz, J. Gallegos, J. L. Sanz, and E. Martínez-González, "Point source detection and extraction from simulated Planck time-ordered data using optimal adaptive filters," *Monthly Notices of the Royal Astronomical Society*, vol. 334, pp. 533–541, Aug. 2002.
- [17] M. López-Cañiego, D. Herranz, R. B. Barreiro, and J. L. Sanz, "A Bayesian approach to filter design: detection of compact sources," in *Computational Imaging II*. Edited by Bouman, Charles A.; Miller, Eric L. *Proceedings of the SPIE, Volume 5299*, pp. 145–154 (2004), ser. Presented at the Society of Photo-Optical Instrumentation Engineers (SPIE) Conference, C. A. Bouman and E. L. Miller, Eds., vol. 5299, May 2004, pp. 145–154.
- [18] M. López-Cañiego, D. Herranz, J. L. Sanz, and R. B. Barreiro, "Detection of Point Sources on Two-Dimensional Images Based on Peaks," *EURASIP Journal on Applied Signal Processing*, vol. 15, pp. 2426–2436, Jul. 2005.
- [19] M. López-Cañiego, D. Herranz, R. B. Barreiro, and J. L. Sanz, "Filter design for the detection of compact sources based on the Neyman-Pearson detector," *Monthly Notices of the Royal Astronomical Society*, vol. 359, pp. 993–1006, May 2005.
- [20] C. L. Bennett, M. Bay, M. Halpern, G. Hinshaw, C. Jackson, N. Jarosik, A. Kogut, M. Limon, S. S. Meyer, L. Page, D. N. Spergel, G. S. Tucker, D. T. Wilkinson, E. Wollack, and E. L. Wright, "The Microwave Anisotropy Probe Mission," *The Astrophysical Journal*, vol. 583, pp. 1–23, Jan. 2003.
- [21] G. Hinshaw, M. R. Nolta, C. L. Bennett, R. Bean, O. Doré, M. R. Greason, M. Halpern, R. S. Hill, N. Jarosik, A. Kogut, E. Komatsu, M. Limon, N. Odegard, S. S. Meyer, L. Page, H. V. Peiris, D. N. Spergel, G. S. Tucker, L. Verde, J. L. Weiland, E. Wollack, and E. L. Wright, "Three-Year Wilkinson Microwave Anisotropy Probe (WMAP) Observations: Temperature Analysis," *The Astrophysical Journal Supplement Series*, vol. 170, pp. 288–334, Jun. 2007.
- [22] J. A. Tauber, "The Planck Mission," in *New Cosmological Data and the Values of the Fundamental Parameters*, ser. IAU Symposium, A. N. Lasenby and A. Wilkinson, Eds., vol. 201, 2005, pp. 86+.
- [23] D. Maino, A. Farusi, C. Baccigalupi, F. Perrotta, A. J. Banday, L. Bedini, C. Burigana, G. De Zotti, K. M. Górski, and E. Salerno, "All-sky astrophysical component separation with Fast Independent Component Analysis (FASTICA)," *Monthly Notices of the Royal Astronomical Society*, vol. 334, pp. 53–68, Jul. 2002.
- [24] D. Maino, S. Donzelli, A. J. Banday, F. Stivoli, and C. Baccigalupi, "Cosmic microwave background signal in Wilkinson Microwave Anisotropy Probe three-year data with FASTICA," *Monthly Notices of the Royal Astronomical Society*, vol. 374, pp. 1207–1215, Feb. 2007.
- [25] K. Maisinger, M. P. Hobson, and A. N. Lasenby, "A maximum entropy method for reconstructing interferometer maps of fluctuations in the cosmic microwave background radiation," *Monthly Notices of the Royal Astronomical Society*, vol. 290, pp. 313–326, Sep. 1997.
- [26] V. Stolyarov, M. P. Hobson, M. A. J. Ashdown, and A. N. Lasenby, "All-sky component separation for the Planck mission," *Monthly Notices of the Royal Astronomical Society*, vol. 336, pp. 97–111, Oct. 2002.
- [27] R. B. Barreiro, M. P. Hobson, A. J. Banday, A. N. Lasenby, V. Stolyarov, P. Vielva, and K. M. Górski, "Foreground separation using a flexible maximum-entropy algorithm: an application to COBE data," *Monthly Notices of the Royal Astronomical Society*, vol. 351, pp. 515–540, Jun. 2004.
- [28] H. K. Eriksen, A. J. Banday, K. M. Górski, and P. B. Lilje, "On Foreground Removal from the Wilkinson Microwave Anisotropy Probe Data by an Internal Linear Combination Method: Limitations and Implications," *The Astrophysical Journal*, vol. 612, pp. 633–646, Sep. 2004.
- [29] F. R. Bouchet and R. Gispert, "Foregrounds and CMB experiments I. Semi-analytical estimates of contamination," *New Astronomy*, vol. 4, pp. 443–479, Sep. 1999.
- [30] D. Herranz, J. L. Sanz, M. P. Hobson, R. B. Barreiro, J. M. Diego, E. Martínez-González, and A. N. Lasenby, "Filtering techniques for the detection of Sunyaev-Zel'dovich clusters in multifrequency maps," *Monthly Notices of the Royal Astronomical Society*, vol. 336, pp. 1057–1068, Nov. 2002.
- [31] J. M. Diego, P. Vielva, E. Martínez-González, J. Silk, and J. L. Sanz, "A Bayesian non-parametric method to detect clusters in Planck data," *Monthly Notices of the Royal Astronomical Society*, vol. 336, pp. 1351–1363, Nov. 2002.
- [32] B. M. Schäfer, C. Pfommer, R. M. Hell, and M. Bartelmann, "Detecting Sunyaev-Zel'dovich clusters with Planck - II. Foreground components and optimized filtering schemes," *Monthly Notices of the Royal Astronomical Society*, vol. 370, pp. 1713–1736, Aug. 2006.
- [33] J.-B. Melin, J. G. Bartlett, and J. Delabrouille, "Catalog extraction in SZ cluster surveys: a matched filter approach," *Astronomy & Astrophysics*, vol. 459, pp. 341–352, Nov. 2006.
- [34] M. Maturi, T. Enßlin, C. Hernández-Monteagudo, and J. A. Rubiño-Martín, "A linear-filter approach to extracting the Rees-Sciama effect in merging clusters of galaxies," *Astronomy & Astrophysics*, vol. 467, pp. 411–419, May 2007.

PLACE
PHOTO
HERE

Diego Herranz received the B.S. degree in 1995 and the M.S. degree in physics from the Universidad Complutense de Madrid, Madrid, Spain, in 1995 and the Ph.D. degree in astrophysics from Universidad de Cantabria, Santander, Spain, in 2002. He was a CMBNET Postdoctoral Fellow at the Istituto di Scienza e Tecnologie dell'Informazione "A. Faedo" (CNR), Pisa, Italy, from 2002 to 2004. He is currently at the Instituto de Física de Cantabria, Santander, Spain, as UC Teaching Assistant. His research interests are in the areas of Cosmic Microwave Background astronomy and extragalactic point source statistics as well as the application of statistical signal processing to astronomical data, including blind source separation, linear and nonlinear data filtering, and statistical modeling of heavy-tailed processes.



PLACE
PHOTO
HERE

José Luis Sanz received the Ph.D. degree in theoretical physics from Universidad Autonoma de Madrid, Spain, in 1976. He was a M.E.C. Postdoctoral Fellow at the Queen Mary College, London, U.K., during 1978. He is currently at the Instituto de Física de Cantabria, Santander, Spain, as UC Professor on Astronomy since 1987. His research interests are in the areas of Cosmic Microwave Background astronomy (anisotropies, non-Gaussianity), extragalactic point sources and clusters of galaxies (blind/non-blind detection, estimation, statistics) as well as the

development of techniques in signal processing (wavelet design, linear/non-linear filters, time-frequency, sparse representations) and application of such tools to astronomical data.